SEISMIC ANALYSIS OF STRUCTURES WITH LOCALIZED NONLINEARITIES

Dennis Row (I)
Vahid Schricker (II)
Presenting Author: Dennis Row

SUMMARY

This paper presents efficient computational algorithms for the seismic analysis of structures with predetermined, localized nonlinearities. Two procedures for dynamic step-by-step analysis have been formulated, using a general substructuring methodology. The methods can be applied to any structural system which can be separated into linear and nonlinear components. A final analysis model is assembled from all the nonlinear finite elements plus any number of linear superelements. The methods are illustrated by case studies on a steel frame with base uplift, and a concrete arch dam with verticle joint opening.

INTRODUCTION

Present earthquake design philosophy recognizes that many structures will be stressed beyond their elastic limits in the event of a major earthquake. An acceptable design is one which will resist a moderate earthquake with no primary structural damage, and survive a catastrophic earthquake without collapse. In the design process, structural elements are proportioned using linear structural analysis, although it is recognized that nonlinear behavior will occur. Adequate performance under severe loadings is engineered using judgment and good structural detailing. Performance during severe earthquakes can be evaluated using nonlinear finite element analysis techniques. However, existing nonlinear techniques are too expensive for use by the practicing professional engineer.

This paper presents results of a study [1], in which efficient methods were developed, for the dynamic seismic response analysis of structures with localized nonlinearities. The physical characteristics of this class of structures are exploited by using substructure concepts in the dynamic response analysis. The linear substructures can be identified and coupled together by a nonlinear substructure [2,3].

Many important structures with such local nonlinearities can be identified. One major class consists of structures which are designed to permit tipping or uplift in response to horizontal earthquake excitation, such as; bridge piers; buildings not anchored against uplift; thin shell metal cylindrical liquid storage tanks with base uplift. An additional category of localized nonlinearity is encountered in structures with joints which may open

(I) President, SSD, Inc., Berkeley, California, USA
(II) Project Engineer, SSD, Inc., Berkeley, California, USA

or close during earthquakes. An important example is a concrete arch dam which is built as a system of independent concrete monoliths separated by vertical joints. Even though these joints are grouted under high pressure to provide continuity under static loading, during dynamic response to an intense earthquake they tend to open. The actual dynamic behavior, and a rational assessment of safety, can be determined only by a nonlinear analysis which accounts for opening and closing of the joints.

NUMERICAL ALGORITHMS

Two step-by-step dynamic integration procedures are presented for structures with localized nonlinearities. Both methods are based on the use of linear and nonlinear substructures. They are much more efficient than standard nonlinear analysis because the element state determination calculations and stiffness matrix reduction operations are limited to the final level nonlinear substructure. The scope of the nonlinear analysis problem is reduced to the size of the nonlinear substructure. The formulation and numerical implementation details of these methods can be found in ref [1]. The methods are summarized as follows.

Exact Method

The major numerical tasks required during a given time step are listed in Table 1. This method is numerically "exact", in that it considers all d.o.f. of the linear substructures. The method is formulated within an overall automatic time step selection strategy. Within a given time step the nonlinear solution is calculated using an event-to-event strategy (step C) which controls load unbalance and makes the analysis automatic. The linear substructures are solved in terms of a transformed variable, $\Delta\underline{x}_j$, which simplifies the calculation of the effective load at each step (see step B1.)

Ritz Method

This method is summarized in Table 2. The method is approximate because it uses Ritz functions, based on the fixed base modes to represent the dynamics of the linear substructure. This method is formulated within the same overall automatic time step strategy, and the procedure at the nonlinear substructure level is identical to the exact method. The Ritz method is particularly useful for systems with very large linear substructures. Such systems can be analysed accurately by considering a small number of generalized d.o.f.

CASE STUDIES

The above methods were illustrated by studies on: (1) A frame structure with base uplift and (2) a concrete arch dam with joint opening. The accuracy of the different procedures is assessed, and the computational efforts (number of numerical operations) are compared.

Frame with Base Uplift

The two-dimensional model of a 9-story, 3-bay steel frame which was studied both experimentally and analytically by Huckelbridge and Clough [4] is

shown in Fig. 1. For the analyses described here, uplift effects were modeled using gap elements. Each element is a nonlinear elastic spring, with finite compressive stiffness and zero tensile stiffness. A compressive stiffness of 500 k/in was assumed, corresponding to a relatively stiff impact pad. The structure is modeled using two substructures, namely a linear substructure consisting of elastic beams and columns (the superstructure), and a nonlinear substructure (the final structure) made up by attaching gap elements at the base. The frame was analyzed for the first 6.2 seconds (before time scaling) of the El Centro, 1940 N-S record, considering only horizontal ground motion. The record was amplified in intensity to produce a peak ground acceleration of 0.912g. For solution stability, the event-to-event solution strategy was used with a constant time step, $\Delta t = 0.01$ sec.

Results from the analyses are shown in Figures 2 through 4. Results using the exact method are identical to those for the fully nonlinear analysis, as expected. The results from the approximate analysis with 10 Ritz vectors are essentially identical to the exact case (see Figs. 2-4). Analyses with different number of Ritz vectors indicated that higher modes of vibration in the superstructure have a significant effect on the gap forces. In particular, the gap forces are affected by vertical high frequency oscillation through the columns. The total numbers of operations for both the exact and the Ritz (10 modes) analyses were 1.0×10^6 and 2.9×10^6, respectively. This is significantly less than the 15.4×10^6 operation for fully nonlinear analysis. The savings result from skipping the state determination calculations in the linear substructure. A comparison of the numbers of operations for the exact and Ritz analyses shows that the exact method requires fewer operations for this example. The advantage of the Ritz method is that fewer operations are required for load reduction and backsubsitution in the linear substructure. This is not a major saving for this example because the number of internal degrees of freedom (d.o.f.) for the linear substructure is small.

Arch Dam with Joint Opening

The Xiang Hong Dain dam is a single-curvature arch dam, built in China, which has been studied analytically by Clough [5] in its linear elastic range. The three-dimensional model used for the present study is shown in Fig. 5. Five vertical planes of contraction joints were assumed, as shown, in each of which joint opening could occur.

Joint opening effects were modeled by zero-length gap elements, with finite stiffness in compression and zero stiffness in tension. The dam body was modeled by 16-node linear elastic 3D solid elements. The rock foundation was assumed to be rigid. The assumption of five vertical joints divides the arch dam into six concrete monoliths, each modeled as a linear substructure. The final structure is assembled by adding gap elements (representing the joint regions) to the six superelements. Hydrostatic loads were initially applied which produced compressive forces in the joints. The dam was then analyzed for the first three seconds of the El Centro 1940 N-S record, applied in the upstream-downstream direction (horizontal Y-direction). The record was amplified in intensity by a factor of 3.0 to produce a peak ground acceleration of 0.96g. The event-to-event solution strategy was used, with a constant time step $\Delta t = 0.01$ sec.

The results from the analysis are shown in Figs 6 through 10. Gap opening occured in all the contraction joints. The largest computed opening was at the dam crest on the upstream face equal to 0.03226 m (more than 1-1/4 in.). The results from the analysis with 5 Ritz vectors are in fairly good agreement with the exact result. Operation counts were performed to compare the computational efforts involved in the exact and Ritz analyses. The exact method requires fewer operations (1.43×10^9 vs. 1.76×10^9). This is because most of the effort is in the large final nonlinear substructure (313 d.o.f. vs. 5 generalized d.o.f. for each linear substructure) which is the same for both methods.

CONCLUSIONS

This paper has presented and demonstrated efficient computational schemes for the seismic analysis of structures with localized nonlinear zones. They allow the analysis and seismic performance assessment of many structures which were previously impractical to analyze. Both the exact and Ritz methods give accuracte solutions to the cases studied, for approximately the same numerical effort. Both methods are much more efficient than standard nonlinear analysis techniques. The Ritz method is particularly efficient for structures with very large linear substructures.

ACKNOWLEDGMENTS

The support of the National Science Foundation, under Grant No. PFR-7922695 is gratefully acknowledged. The authors wish to express their appreciation to Professor R. W. Clough for his interest and advice throughout this project.

REFERENCES

1. Row, D. G. and Schricker, V. "Analysis of Earthquake Induced Response for Structures with Localized Nonlinearities", Report to National Science Foundation, SSD, Inc., Berkeley, February 1983.
2. Row, D. G. and Powell, G. H., "A Substructure Technique for Nonlinear Static and Dynamic Analysis," Report No. UCB/EERC 78-15, University of California, Berkeley, August 1978.
3. Clough, R. W. and Wilson, E. L., "Dynamic Analysis of Large Structural Systems with Local Nonlinearities," presented at the International Conference on Finite Element Methods in Nonlinear Mechanics, Institut fur Statik und Dynamik, Universitt of Stuttgart, August 30 to September 1978.
4. Huckelbridge, A. and Clough, R. W., "Shaking Table Tests of Building Frame Permitted to Uplift," Journal of the Structural Division, ASCE, Vol. 104, No. ST8, August 1978.
5. Private communication with R. W. Clough, University of California, Berkeley, 1983.

TABLE 1 EXACT METHOD

CALCULATIONS TO BE PERFORMED IN TIME STEP j, (Δt_j) FOR EVENT-TO-EVENT STRATEGY WITH AUTOMATIC TIME STEP SELECTION

A. LINEAR SUBSTRUCTURES - STIFFNESS FORMATION AND REDUCTION - [Performed initially and at changes in time step]

1. Form Effective Stiffness Matrix - [Damping; $\underline{C} = \alpha\underline{M} + \beta\underline{K}$]

$$\hat{\underline{K}} = \begin{bmatrix} \hat{\underline{K}}_{ii} & \hat{\underline{K}}_{ir} \\ \hat{\underline{K}}_{ri} & \hat{\underline{K}}_{rr} \end{bmatrix} = (a_1 + \alpha a_4)\underline{M} + (1 + \beta a_4)\underline{K}; \text{ where } a_1 = \frac{1}{\beta_n \Delta t_j^2},\ a_2 = \frac{1}{\beta_n \Delta t_j},\ a_3 = \frac{1}{2\beta_n},\ a_4 = \frac{\gamma}{\beta_n \Delta t_j},\ a_5 = \frac{\gamma}{\beta_n},\ a_6 = \frac{\gamma}{2\beta_n} - 1$$

2. Reduce to Superelement D.O.F.

$\hat{\underline{K}}_R = \hat{\underline{K}}_{rr} - \hat{\underline{K}}_{ri}\,\hat{\underline{K}}_{ii}^{-1}\,\hat{\underline{K}}_{ir}$ = Reduced Effective Stiffness

B. LINEAR SUBSTRUCTURES - EFFECTIVE LOAD REDUCTION - [Performed at all steps]

1. Form Effective Dynamic Load Increment - [in transformed variable, $\Delta\underline{x}_j$]

$$\hat{\underline{P}}_j = \begin{bmatrix} \hat{\underline{P}}_i \\ \hat{\underline{P}}_r \end{bmatrix}_j = \underline{R}_j^E + \underline{M}(B_1\underline{r}_{j-1} + \dot{B}_2\underline{r}_{j-1} + B_3\ddot{\underline{r}}_{j-1}); \text{ where } B_1 = \frac{a_1+\alpha a_4}{1+\beta a_4};\ B_2 = a_2 + \alpha(a_5-1) - \beta(a_5-1)B_1;\ B_3 = a_3 + \alpha a_6 - 1 - \beta a_6 B_1$$

2. Reduce to Superelement D.O.F.

$\hat{\underline{P}}_{Rj} = \hat{\underline{P}}_{rj} - \hat{\underline{K}}_{ri}\,\hat{\underline{K}}_{ii}^{-1}\,\hat{\underline{K}}_{ir}\,\hat{\underline{P}}_{ij}$

3. Transform to Standard Displacement Variable - [$\Delta\underline{r}_j = \Delta\underline{x}_j - (b_1\underline{r}_{j-1} + b_2\dot{\underline{r}}_{j-1} + b_3\ddot{\underline{r}}_{j-1})$]

$\hat{\underline{R}}_{Rj} = \hat{\underline{P}}_{Rj} - \hat{\underline{K}}_R\,(b_1 r_{j-1} + b_2\,\dot{r}_{j-1} + b_3\ddot{r}_{j-1})_r$; where $b_1 = \frac{1}{1+\beta a_4}$; $b_2 = \frac{-\beta(a_5-1)}{1+\beta a4}$; $b_3 = \frac{-\beta a_6}{1+\beta a_4}$

C. NONLINEAR SUBSTRUCTURE - [Event-to-Event Solution Strategy; Performed at all steps]

1. Form Total Step Load

$$\Delta\hat{\underline{R}}_j = \Delta\underline{R}_j^E + \underline{R}_{ij} + \Delta\underline{R}_{j-1} + \sum_{1}^{\ell \text{ sub}} \hat{\underline{R}}_{Rj}; \text{ where } \Delta\underline{R}_{j-1} = \underline{M}(a_2\dot{\underline{r}}_{j-1} + a_3\ddot{\underline{r}}_{j-1}) + \underline{C}_j(a_5\dot{\underline{r}}_{j-1} + a_6\ddot{\underline{r}}_{j-1})$$

2. Solve for Incremental Displacement Using Event-to-Event Strategy - [Perform for event substeps; n = 1, 2, ..., m]

a. Form Total Current Tangent Stiffness

$$\hat{\underline{K}}_{nj} = {}_n\underline{K}_j + \sum_{1}^{\ell \text{ sub}} \hat{\underline{K}}_R; \text{ where } {}_n\underline{K}_j = \text{nonlinear substructure tangent stiffness at step j, substep n.}$$

b. Solve for Substep n Displacement Increment

$$\hat{\underline{K}}_{nj}\,\Delta\underline{r}_{nj} = f_n \prod_{k=1}^{n-1}(1-f_k)\ \Delta\hat{\underline{R}}_j; \text{ where } f_k = \text{event factor for substep k, and } \Pi \text{ indicates the product}$$

c. Accumulate Displacement Increment $\Delta\underline{r}_j = \Delta\underline{r}_j + {}_n\Delta\underline{r}_j$

D. LINEAR SUBSTRUCTURE - DISPLACEMENT RECOVERY - [Performed at all steps]

1. Transform Superelement Displacements $\Delta\underline{r}_{jr}$ to $\Delta\underline{x}_{jr}$

$\Delta\underline{x}_{jr} = \Delta\underline{r}_{jr} + (b_1\underline{r}_{j-1} + b_2\dot{\underline{r}}_{j-1} + b_3\ddot{\underline{r}}_{j-1})_r$

2. Backsubstitute for $\Delta\underline{x}_{ji}$

$\Delta\underline{x}_{ji} = \hat{\underline{K}}_{ii}^{-1}\,(\hat{\underline{P}}_{ij} - \hat{\underline{K}}_{ir}\,\Delta\underline{x}_{jr})$

3. Calculate Increments in Displacement, Velocity and Acceleration

$\Delta\underline{r}_j = \Delta\underline{x}_j - (b_1\underline{r}_{j-1} + b_2\dot{\underline{r}}_{j-1} + b_3\ddot{\underline{r}}_{j-1})$; $\Delta\dot{\underline{r}}_j = a_1\Delta\underline{r}_j - (a_5\dot{\underline{r}}_{j-1} + a_6\ddot{\underline{r}}_{j-1})$; $\Delta\ddot{\underline{r}}_j = a_4\Delta\underline{r}_j - (a_2\dot{\underline{r}}_{j-1} + a_3\ddot{\underline{r}}_{j-1})$

NEXT STEP

Return to A. Based on midstep error norm do one of following:

1) Continue with current step size, or; 2) Continue with increased step size; or; 3) Repeat with reduced step size

TABLE 2 RITZ METHOD

CALCULATIONS TO BE PERFORMED IN TIME STEP j, (Δt_j) FOR EVENT-TO-EVENT STRATEGY WITH AUTOMATIC TIME STEP SELECTION

A. LINEAR SUBSTRUCTURE - RITZ REDUCTION - [Performed once prior to step-by-step analysis]

1. Form Stiffness and Mass Matrices

$$\underline{K} = \begin{bmatrix} \underline{K}_{ii} & \underline{K}_{ir} \\ \underline{K}_{ri} & \underline{K}_{rr} \end{bmatrix} ; \quad \underline{M} = \begin{bmatrix} M_{ii} & 0 \\ 0 & M_{rr} \end{bmatrix} = \text{diag.}$$

2. Solve for Lowest Fixed Base Modes

$$\underline{K}_{ii}\,\underline{\Phi}_n = \underline{M}_{ii}\,\underline{\Phi}_n$$

3. Form Coordinate Transformation and Reduced Matrices

$$\begin{bmatrix} \underline{r}_i \\ \underline{r}_r \end{bmatrix} = \begin{bmatrix} \underline{\Phi}_n & \underline{K}_{ii}^{-1}\underline{K}_{ir} \\ 0 & \underline{I} \end{bmatrix} \begin{bmatrix} \underline{r}_n \\ \underline{r}_r \end{bmatrix} \rightarrow \underline{r} = \underline{T}\,\underline{r}^* ; \; \underline{K}^* = \underline{T}^T\,\underline{K}\,\underline{T} ; \; \underline{M}^* = \underline{T}^T\underline{M}\,\underline{T} \qquad r^* = \text{Generalized displacements}$$

B. LINEAR SUBSTRUCTURE - EFFECTIVE REDUCED STIFFNESS FORMATION AND REDUCTION - [Initially and at changes in time step]

1. Form Effective Stiffness Matrix - [Damping; $\underline{c}^* = \alpha\underline{M}^* + \beta\underline{K}^*$]

$$\underline{K}^* = \begin{bmatrix} \hat{\underline{K}}^*_{nn} & \hat{\underline{K}}^*_{nr} \\ \hat{\underline{K}}^*_{rn} & \hat{\underline{K}}^*_{rr} \end{bmatrix} = (a_1 + \alpha a_4)\,\underline{M}^* + (1 + \beta a_4)\underline{K}^*$$

2. Reduce to Superelement D.O.F.

$$\hat{\underline{K}}^*_R = \hat{\underline{K}}^*_{rr} - \hat{\underline{K}}^*_{rn}\,\hat{\underline{K}}^{*-1}_{nn}\,\hat{\underline{K}}^*_{nr}$$

C. LINEAR SUBSTRUCTURES - EFFECTIVE LOAD TRANSFORMATION AND REDUCTION - [Performed at all steps]

1. Form Effective Dynamic Load Increment

$$\hat{\underline{R}}^*_j = \begin{bmatrix} \hat{\underline{R}}^*_n \\ \hat{\underline{R}}^*_r \end{bmatrix}_j = \underline{T}^T\,\underline{R}^E_j + M^*\left[(a_3 + \alpha a_6 - 1)\ddot{\underline{r}}^*_{j-1} + (a_2 + \alpha a_5 - \alpha)\dot{\underline{r}}^*_{j-1}\right] + \underline{K}^*\left[\beta a_6\,\ddot{\underline{r}}^*_{j-1} + \beta(a_5 - 1)\dot{\underline{r}}^*_{j-1} - \underline{r}^*_{j-1}\right]$$

D. NONLINEAR SUBSTRUCTURE - [Event-to-Event Solution Strategy Performed at all steps]

Same as Section C in Table 1, with $\hat{K}^*_R$ replacing $\hat{K}_R$, and $\hat{R}^*_{Rj}$ replacing $\hat{R}_{Rj}$

E. LINEAR SUBSTRUCTURE - GENERALIZED DISPLACEMENT RECOVERY - [Performed at all steps]

1. Backsubstitute for Δr_{jn}

$$\Delta\underline{r}_{jn} = \hat{\underline{K}}^{*-1}_{nn}\,(\hat{\underline{R}}^*_{nj} - \hat{\underline{K}}_{nr}\,\Delta\underline{r}_{jr})$$

2. Calculate Increments in Generalized Velocity and Acceleration

$$\Delta\dot{\underline{r}}^*_j = a_1\,\underline{r}^*_j - (a_5\dot{\underline{r}}^*_{j-1} + a_6\ddot{\underline{r}}^*_{j-1}) \; ; \; \Delta\ddot{\underline{r}}^*_j = a_4\Delta\underline{r}^*_j - (a_2\dot{\underline{r}}^*_{j-1} + a_3\ddot{\underline{r}}^*_{j-1})$$

F. NEXT STEP

Return to B. Based on midstep error norm do one of following:

1) Continue with current step size, or; 2) Continue with increased step size, or; 3) Repeat with reduced step size

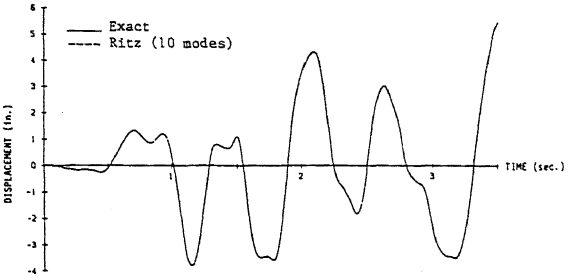

FIG. 2 COMPARISON OF ROOF DISPLACEMENTS

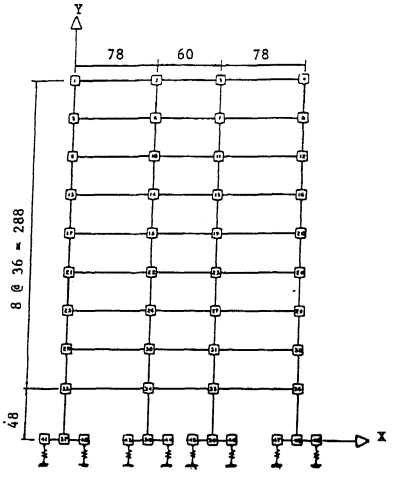

FIG. 1 FRAME MODEL

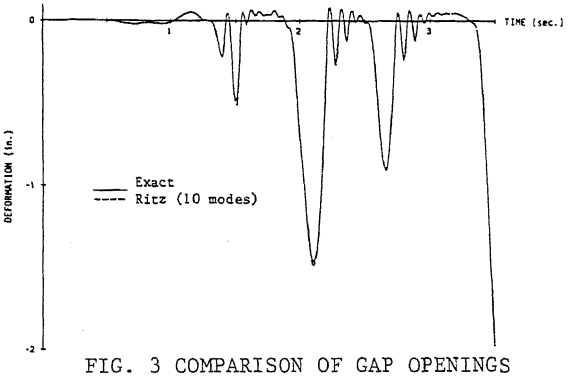

FIG. 3 COMPARISON OF GAP OPENINGS AT LEFT COLUMN

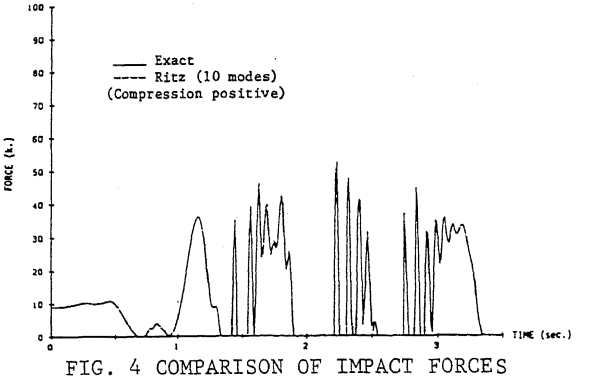

FIG. 4 COMPARISON OF IMPACT FORCES AT LEFT COLUMN

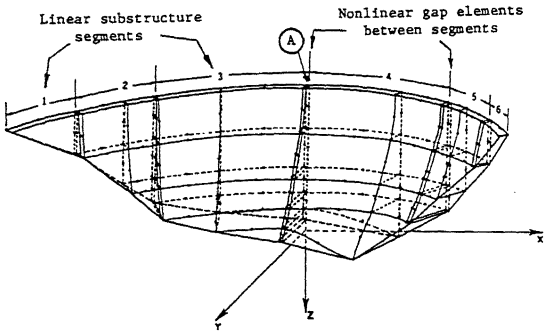

FIG. 5 ARCH DAM MODEL

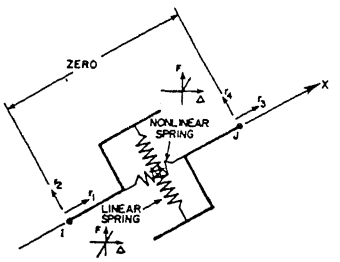

FIG. 6 GAP ELEMENT

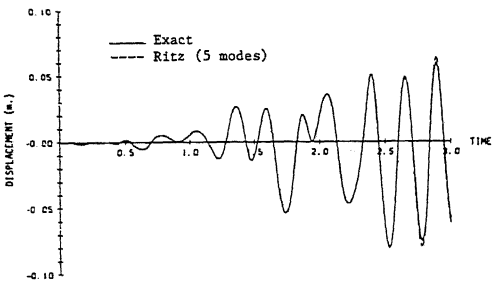

FIG. 7 COMPARISON OF Y-DISPLACEMENTS AT (A)

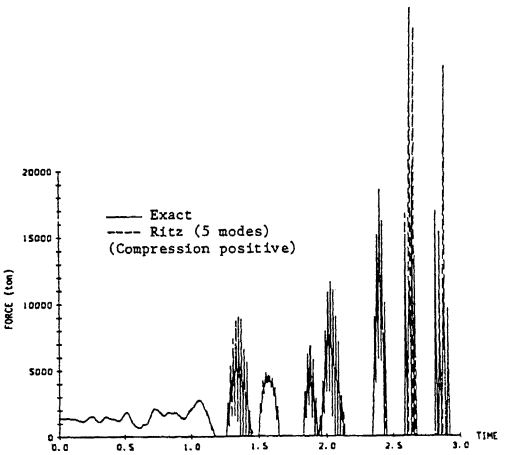

FIG. 8 COMPARISON OF DOWNSTREAM GAP IMPACT FORCES AT (A)

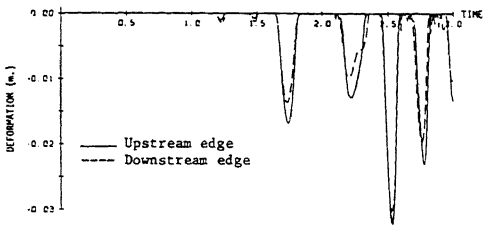

FIG. 9 GAP OPENINGS AT (A) (EXACT ANALYSIS)

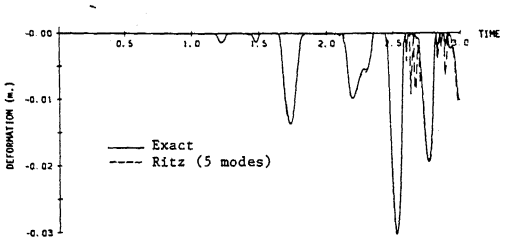

FIG. 10 COMPARISON OF DOWNSTREAM GAP OPENINGS AT (A)